Heat and Mass Transfer 34 (1998) 307–316 © Springer-Verlag 1998

2D numerical simulation for simultaneous heat, water and gas migration in soil bed under different environmental conditions

W. Liu, X. X. Zhao, K. Mizukami

Abstract A general mathematical model for investigating simultaneous heat, water and gas (air plus vapor) transfer in unsaturated porous soil under different environmental conditions is presented based on the volume-averaging method. Two-dimensional numerical simulation in steady state is conducted for obtaining accurate images of field characteristics in a confined soil bed, which might be useful to provide necessary information for agricultural applications. Various effects of environmental parameters, such as ambient temperature, relative humidity, radiative heat flux and wind speed, on transport processes in soil without plant roots are analyzed through the calculating results in the present paper.

List of symbols

A	area, m^2
c	specific heat, $J/(Kg \cdot K)$
D_l	diffusivity of water in porous medium, m^2/s
D_v	molecular diffusivity of vapor in air, m^2/s
D_{Tv}	diffusivity defined in Eq. (11), $m^2/(s \cdot K)$
D_{lv}	diffusivity defined in Eq. (11), m^2/s
g	acceleration of gravity m/s^2
h	convection heat transfer coefficient, $W/(m^2 \cdot K)$
h_m	convection mass transfer coefficient, m/s
H	Vertical height in y-direction of soil bed, m
I	incident solar radiation, W/m^2
k_m	apparent thermal conductivity, $W/(m \cdot K)$
k_g	equivalent permeability of gas-mixture, m^2
k_l	unsaturated permeability of liquid, m^2
K_g	infiltrating conductivity of gas-mixture, m/s
K_l	hydraulic conductivity of liquid, m/s
L	horizontal width in x-direction of soil bed, m
$\dot{m}$	mass rate of phase change, $Kg/(m^3 \cdot s)$
P	pressure, Pa
S_r	source term related to root-absorbed moisture, $Kg/(m^3 \cdot s)$
t	time, s
T	temperature, K(°C)
T_0	reference temperature defined in Eq. (5), K(°C)
u	velocity component in x-direction, m/s
v	velocity component in y-direction, m/s
V	averaging volume, m^3
$\vec{V}$	velocity vector, m/s

Greek symbols

α	representing liquid-, gas- or solid-phase
β	thermal expansion coefficient, 1/K
γ	latent heat, J/Kg
ε	phase content, %
μ	viscosity, $Kg/(m \cdot s)$
ν	kinematic viscosity, m^2/s
ρ	density, Kg/m^3
σ	Stefan-Boltzman constant, $W/(m^2 \cdot K^4)$
ϕ	porosity, %
Φ_r	source term related to root-absorbed heat, W/m^2
ψ	general definition for physical quantity

Subscripts and superscripts

a	air, ambient
g	gaseous mixture
l	liquid
m	mean, mass
r	root
s	solid, sky
v	vapor

Received on 13 January 1998

W. Liu, X. X. Zhao
Department of Power Engineering
Huazhong University of Science and Technology
Wuhan 430074, P. R. China

K. Mizukami
Department of Mechanical Engineering
Ehime University
Matsuyama 790, Japan

Correspondence to: W. Liu

1 Introduction

As a kind of unsaturated porous media, soil is consisted of solid particles, liquid water, gaseous mixture of vapor and air and other chemical and biological substances. As multiphase flow, evaporation and condensation are involved in transport processes of mass, momentum and energy, modeling and simulating simultaneous heat and mass transfer in soil seems to be rather complicated. A great deal agriculture and engineering applications lead to a so strong background for profound researches on this interesting issue, that many scientists and engineers have contributed a lot of academic and art work to the theoretical and experimental developments in moisture porous soil for the past decades. For plant growth, as an example, level of temperature, maintenance of water and presence of

gas in cultivable soil are very important aspects to management and control of agricultural processes which are closely related to seasons and weather conditions. Well knowledge of thermal and dynamic process in soil under different atmospheric environments may help to result a good solution to the problem of raising productivity for crops.

Compared with the porous media saturated with single fluid, much more physical mechanisms in transport process are involved in the unsaturated moisture soil. Very pioneering theories had been well established by Philip and DeVries [1], Luikov [2], Slattery [3] and Whitaker [4], and also may typical problems in unsaturated porous media had been properly solved with theoretical and experimental developments by scientists [5–8]. However, there still exist some theoretical aspects to be improved and some application areas to be explored. The recent researches in the soil area were reported by references [9–12], but most of them dealt with one-dimensional problems, and considered no motion of air-vapor mixture in soil. The present study is aimed to analyze field variables, as many as possible, in the confined soil bed with two-dimensional distributions, especially influenced by some main ambient factors that are changeable in the numerical simulations.

2
Mathematical formulation

We have established a mathematical modeling in the way of general conservation [13], which may be more suitable than Darcy's motion equation for describing momentum transport phenomena in unsaturated porous media. Darcy's law, as we know, was originally derived on the base of liquid-saturated porous medium, which implies that any kind of extended or revised models for its applications in unsaturated porous media could cause considerable deviation from the original problems, not like in saturated ones. As a matter of fact, Darcy's effect that appears with respect to a Darcy's term in the momentum equation, for our case, surely decays to one of the multimechanisms that dominate the momentum motions both for liquid and gas phases by assemble effects, instead of mainly depending on Darcy's one.

2.1
Governing equations

In disclosing the physical mechanisms of above mentioned phenomena in the moisture soil by the conservational differential equations, some basic assumptions should be made as follows:

1. Homogeneous and isotropic medium with no distension or contraction;
2. Subject to local thermal equilibrium throughout the analysis domain;
3. Liquid phase and gas phase in funicular (continuous) states respectively;
4. Valid for Boussinesq's approximation in gaseous natural convection;
5. Ideal-gas treatment for gaseous mixture in porespace of porous matrix.

2.1.1
Continuity

For water liquid:

$$\frac{\partial\left(\langle\rho_{\mathrm{l}}\rangle^{\mathrm{l}}\varepsilon_{\mathrm{l}}\right)}{\partial t}+\nabla\cdot\left(\langle\rho_{\mathrm{l}}\rangle^{\mathrm{l}}\varepsilon_{\mathrm{l}}\langle\vec{V}_{\mathrm{l}}\rangle^{\mathrm{l}}\right)=-\langle\dot{m}_{\mathrm{l}}\rangle-\langle S_{\mathrm{r,l}}\rangle \tag{1}$$

For gaseous mixture:

$$\frac{\partial\left(\langle\rho_{\mathrm{g}}\rangle^{\mathrm{g}}\varepsilon_{\mathrm{g}}\right)}{\partial t}+\nabla\cdot\left(\langle\rho_{\mathrm{g}}\rangle^{\mathrm{g}}\varepsilon_{\mathrm{g}}\langle\vec{V}_{\mathrm{g}}\rangle^{\mathrm{g}}\right)=\langle\dot{m}_{\mathrm{g}}\rangle-\langle S_{\mathrm{r,g}}\rangle \tag{2}$$

For water vapor:

$$\frac{\partial\left(\langle\rho_{\mathrm{v}}\rangle^{\mathrm{g}}\varepsilon_{\mathrm{g}}\right)}{\partial t}+\nabla\cdot\left(\langle\rho_{\mathrm{v}}\rangle^{\mathrm{g}}\varepsilon_{\mathrm{g}}\left(\langle\vec{V}_{\mathrm{v}}\rangle^{\mathrm{g}}+\langle\vec{V}_{\mathrm{g}}\rangle^{\mathrm{g}}\right)\right)=\langle\dot{m}_{\mathrm{v}}\rangle-\langle S_{\mathrm{r,v}}\rangle \tag{3}$$

2.1.2
Momentum

For liquid phase:

$$\begin{aligned}&\varepsilon_{\mathrm{l}}\frac{\partial\left(\langle\rho_{\mathrm{l}}\rangle^{\mathrm{l}}\langle\vec{V}_{\mathrm{l}}\rangle^{\mathrm{l}}\right)}{\partial t}+\varepsilon_{\mathrm{l}}\left(\langle\vec{V}_{\mathrm{l}}\rangle^{\mathrm{l}}\cdot\nabla\right)\left(\langle\rho_{\mathrm{l}}\rangle^{\mathrm{l}}\langle\vec{V}_{\mathrm{l}}\rangle^{\mathrm{l}}\right)-\langle\dot{m}_{\mathrm{l}}\rangle\langle\vec{V}_{\mathrm{l}}\rangle^{\mathrm{l}}\\&=-\frac{\mu_{\mathrm{l}}D_{\mathrm{l}}\varepsilon_{\mathrm{l}}}{k_{\mathrm{l}}}\nabla\varepsilon_{\mathrm{l}}-\frac{\mu_{\mathrm{l}}\varepsilon_{\mathrm{l}}}{k_{\mathrm{l}}}\langle\vec{V}_{\mathrm{l}}\rangle^{\mathrm{l}}+\mu_{\mathrm{l}}\varepsilon_{\mathrm{l}}\nabla^{2}\langle\vec{V}_{\mathrm{l}}\rangle^{\mathrm{l}}-\langle\rho_{\mathrm{l}}\rangle^{\mathrm{l}}\varepsilon_{\mathrm{l}}\vec{g}\\&\quad-\frac{\mu_{\mathrm{g}}\varepsilon_{\mathrm{g}}}{k_{\mathrm{g}}}\left(\langle\vec{V}_{\mathrm{l}}\rangle^{\mathrm{l}}+\langle\vec{V}_{\mathrm{g}}\rangle^{\mathrm{g}}\right)\end{aligned} \tag{4}$$

For gaseous phase:

$$\begin{aligned}&\varepsilon_{\mathrm{g}}\frac{\partial\left(\langle\rho_{\mathrm{g}}\rangle^{\mathrm{g}}\langle\vec{V}_{\mathrm{g}}\rangle^{\mathrm{g}}\right)}{\partial t}+\varepsilon_{\mathrm{g}}\left(\langle\vec{V}_{\mathrm{g}}\rangle^{\mathrm{l}}\cdot\nabla\right)\left(\langle\rho_{\mathrm{g}}\rangle^{\mathrm{g}}\langle\vec{V}_{\mathrm{g}}\rangle^{\mathrm{g}}\right)+\\&\langle\dot{m}_{\mathrm{g}}\rangle\left(\langle\vec{V}_{\mathrm{g}}\rangle^{\mathrm{g}}+\langle\vec{V}_{\mathrm{v}}\rangle^{\mathrm{g}}\right)=-\varepsilon_{\mathrm{g}}\nabla\langle P_{\mathrm{g}}\rangle^{\mathrm{g}}-\frac{\mu_{\mathrm{g}}\varepsilon_{\mathrm{g}}}{k_{\mathrm{g}}}\left(\langle\vec{V}_{\mathrm{g}}\rangle+\langle\vec{V}_{\mathrm{l}}\rangle\right)\\&+\mu_{\mathrm{g}}\varepsilon_{\mathrm{g}}\nabla^{2}\langle\vec{V}_{\mathrm{g}}\rangle^{\mathrm{g}}-\langle\rho_{\mathrm{g}}\rangle^{\mathrm{g}}\varepsilon_{\mathrm{g}}\vec{g}\beta(\langle T\rangle-T_{0})\end{aligned} \tag{5}$$

2.1.3
Energy

$$\begin{aligned}&\frac{\partial((\rho c)_{\mathrm{m}}\langle T\rangle)}{\partial t}+c_{\mathrm{l}}\varepsilon_{\mathrm{l}}\langle\vec{V}_{\mathrm{l}}\rangle^{\mathrm{l}}\cdot\nabla(\langle\rho_{\mathrm{l}}\rangle^{\mathrm{l}}\langle T\rangle)+c_{\mathrm{g}}\varepsilon_{\mathrm{g}}\langle\vec{V}_{\mathrm{g}}\rangle^{\mathrm{g}}\cdot\nabla\\&(\langle\rho_{\mathrm{g}}\rangle^{\mathrm{g}}\langle T\rangle)+c_{\mathrm{v}}\varepsilon_{\mathrm{g}}(\langle\vec{V}_{\mathrm{g}}\rangle^{\mathrm{g}}+\langle\vec{V}_{\mathrm{v}}\rangle^{\mathrm{g}})\cdot\nabla(\langle\rho_{\mathrm{v}}\rangle^{\mathrm{g}}\langle T\rangle)\\&\quad+c_{\mathrm{l}}\langle T\rangle\langle\vec{V}_{\mathrm{l}}\rangle^{\mathrm{l}}\cdot\nabla(\langle\rho_{\mathrm{l}}\rangle^{\mathrm{l}}\varepsilon_{\mathrm{l}})+c_{\mathrm{g}}\langle T\rangle\langle\vec{V}_{\mathrm{g}}\rangle^{\mathrm{g}}\cdot\nabla(\langle\rho_{\mathrm{g}}\rangle^{\mathrm{g}}\varepsilon_{\mathrm{g}})\\&\quad+c_{\mathrm{v}}\langle T\rangle(\langle\vec{V}_{\mathrm{g}}\rangle^{\mathrm{g}}+\langle\vec{V}_{\mathrm{v}}\rangle^{\mathrm{g}})\cdot\nabla(\langle\rho_{\mathrm{v}}\rangle^{\mathrm{g}}\varepsilon_{\mathrm{g}})\\&=\nabla\cdot(k_{\mathrm{m}}\nabla\langle T\rangle)-\gamma\langle\dot{m}_{l}\rangle-\langle\Phi_{\mathrm{r}}\rangle\end{aligned} \tag{6}$$

2.2
About governing equations

It seems that the present mathematical modeling is much sophisticated, some discussions, therefore, might be necessary for the above governing equations.

1. The volume averaged equations are obtained by introducing a spatial average volume V for including every substantial phase and an intrinsic average volume V_{α} for an individual phase α, and defining the following volume-averaged quantities everywhere in the unsaturated porous body [4].

$$\langle\psi\rangle = \frac{1}{V}\int_V \psi \, dV \tag{7}$$

$$\langle\psi_\alpha\rangle = \frac{1}{V}\int_V \psi_\alpha \, dV = \frac{1}{V}\int_{V_\alpha} \psi_\alpha \, dV \tag{8}$$

$$\langle\psi_\alpha\rangle^\alpha = \frac{1}{V_\alpha}\int_V \psi_\alpha \, dV = \frac{1}{V_\alpha}\int_{V_\alpha} \psi_\alpha \, dV \tag{9}$$

From Eqs. (7–9), one may find that we are only interested in the phase average of a physical quantity in its intrinsic phase space, while its value in other phases is zero. And from those equations, an useful relation between spatial average and intrinsic phase average is gotten in order for deriving the governing equations.

$$\langle\psi_\alpha\rangle = \varepsilon_\alpha\langle\psi_\alpha\rangle^\alpha \tag{10}$$

2. The vapor-diffusion motion in the porous soil plays an important role not only for the mass and energy conservation in phase-change transport process, but also for the momentum conservation, and as the results, it should be involved in the corresponding governing Eqs. (3), (5) and (6) as the form of

$$\langle\vec{V}_v\rangle^g = -D_{Tv}\nabla\langle T\rangle - D_{lv}\nabla\varepsilon_l \ . \tag{11}$$

We prefer here to connect vapor diffusive velocity with temperature and liquid water content that is a basic variable for current numerical simulation. The diffusivity coefficient in Eq. (11) are computable by the formulas according to our previous derivation [14]. In addition, under the assumption of continuous gas phase, the principle of partial pressure law could be introduced in the mathematical modeling, that is to say: $P_a + P_v = P_g$ and $\varepsilon_a = \varepsilon_v = \varepsilon_g$, by which the vapor migration behavior could be evaluated through the equations mentioned above without involving any air-related quantities.

3. The apparent physical properties of unsaturated porous soil are simply set to the mean ones, say $(\rho c)_m = \varepsilon_s\rho_s c_s + \varepsilon_l\rho_l c_l + \varepsilon_g\rho_g c_g$ and $k_m = \varepsilon_s k_s + \varepsilon_l k_l + \varepsilon_g k_g$. The equivalent infiltrating conductivity of gas-mixture K_g, corresponding to hydraulic conductivity of liquid K_l, was defined from our previous work [15], which is associated with permeability $K_g = k_g g/\nu_g$ as the same form in liquid phase $K_l = k_l g/\nu_l$.

4. The relative motions between water vapor and gaseous mixture, are taken into account in the present model, because the diffusive migration of water vapor may be inverse to the bulk motion of gaseous mixture that could form vortexes in the situation of current confined boundaries. As the results, the sign of relative velocity terms, positive or negative, in the above equations depends on the individual point of domain. The relative motion between water liquid and gaseous mixture is also considered in the Darcy's resistance terms of Eqs. (4, 5), which is available for quantitative evaluation based on the definition of K_g.

5. As one may see, in continuity and energy equations, some special source terms [16] appear for representing the moisture and the heat absorbed by the plant roots that take the moisture in soil from two different tunnels: water liquid source $\langle S_{r,l}\rangle$ and water vapor source $\langle S_{r,v}\rangle = \langle S_{r,g}\rangle$,

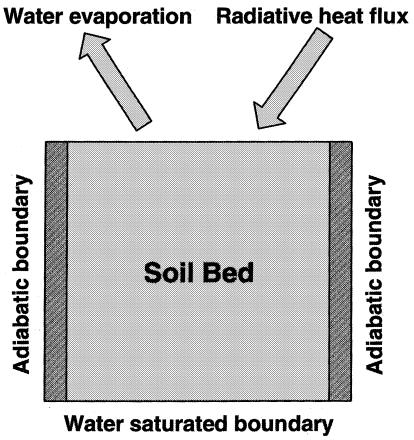

Fig. 1. A confined soil bed with its boundaries

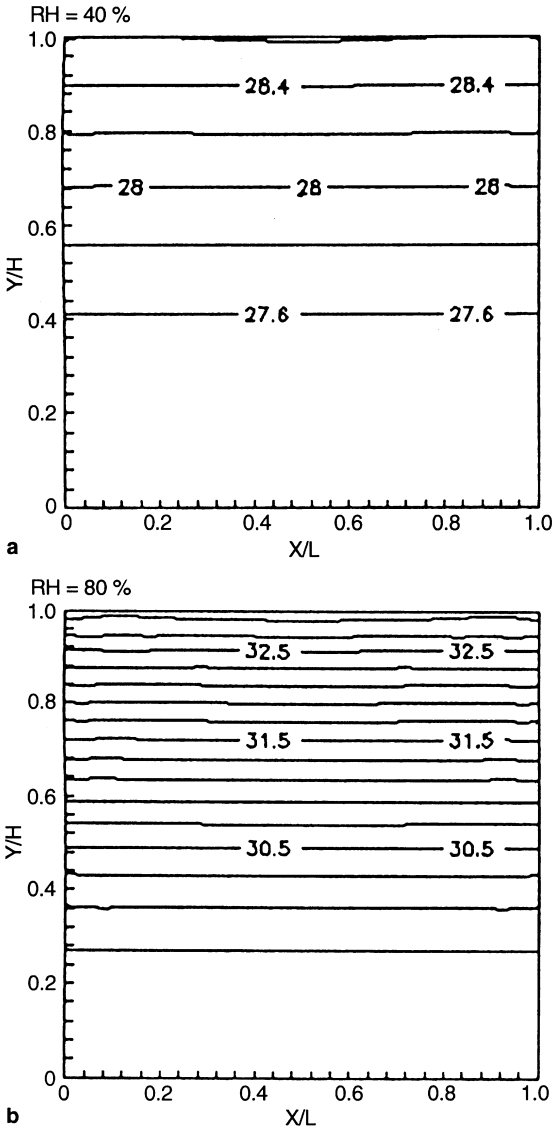

Fig. 2a,b. Temperature contour line (°C) (Ta = 30 °C, I = 400 W/m^2, Va = 1 m/s)

which are from water evaporation of the gas-liquid interfaces inside porous body, and subject to mass continuity $\langle\dot{m}_v\rangle = \langle\dot{m}_g\rangle = \langle\dot{m}_l\rangle$. Source term $\langle\Phi_r\rangle$ indicates the root-

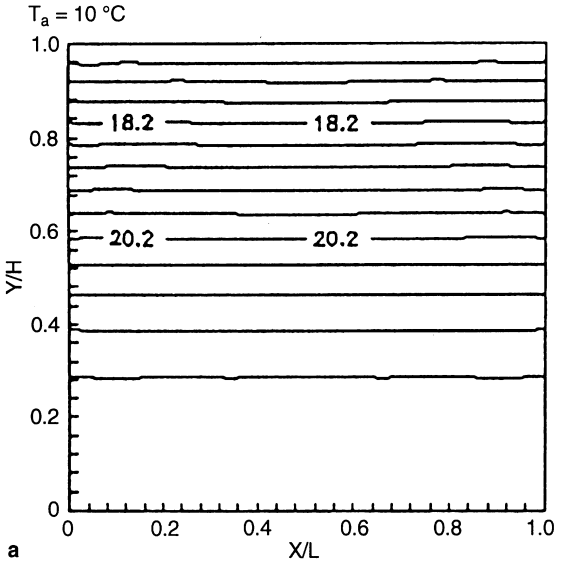

Fig. 3. Temperature contour line (°C) (RH = 60% , I = 400 W/m^2, Va = 1 m/s)

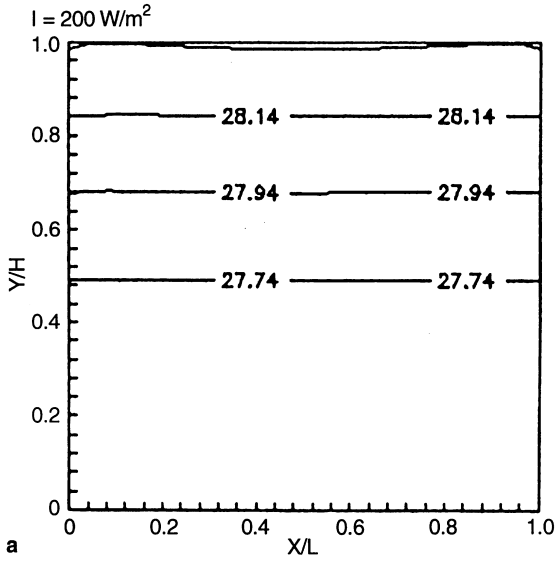

Fig. 4. Temperature contour line (°C) (RH = 60%, Ta = 30 °C, Va = 1 m/s)

absorbed heat that is a very important condition for the plant growth, however, seldom considered by theoretical models so far. But in the numerical simulation under current investigation, we simply drop those source terms from the continuity and the energy equations in the case of non-planting soil bed.

6. For the research fields in dynamic and thermal soil science, the most models and their numerical solutions are popular in one-dimension formulations that well fit the width soil area, but not suitable for the confined soil bed. Although our attentions are focused on the transport phenomena which occur in the way of multi-dimension process, the present mathematical model can be easily reduced to any one-dimensional calculation for such a case of actual agriculture application, by changing the soil bed boundaries to infinite in two horizontal coordinates. By the way, this theoretical modeling is just for the unsaturated moisture soil, but can be modified to a two-region model by dropping the liquid momentum equation, and applying the diffusive equation in the dry region.

2.3 Boundary conditions

The soil bed and its thermal and dynamic boundaries under investigation are illustrated in Fig. 1. All boundary conditions that can also reflect the structure of setup, in coincidence with our late experimental soil bed, are stated as follows:

$$x = 0: \quad \frac{\partial T}{\partial x} = 0, \quad u_l = u_g = v_l = v_g = 0; \tag{12}$$

$$x = L: \quad \frac{\partial T}{\partial x} = 0, \quad u_l = u_g = v_l = v_g = 0; \tag{13}$$

$$y = 0: \quad \frac{\partial T}{\partial y} = 0, \quad u_l = u_g = v_l = v_g = 0, \quad \varepsilon_g = 0; \tag{14}$$

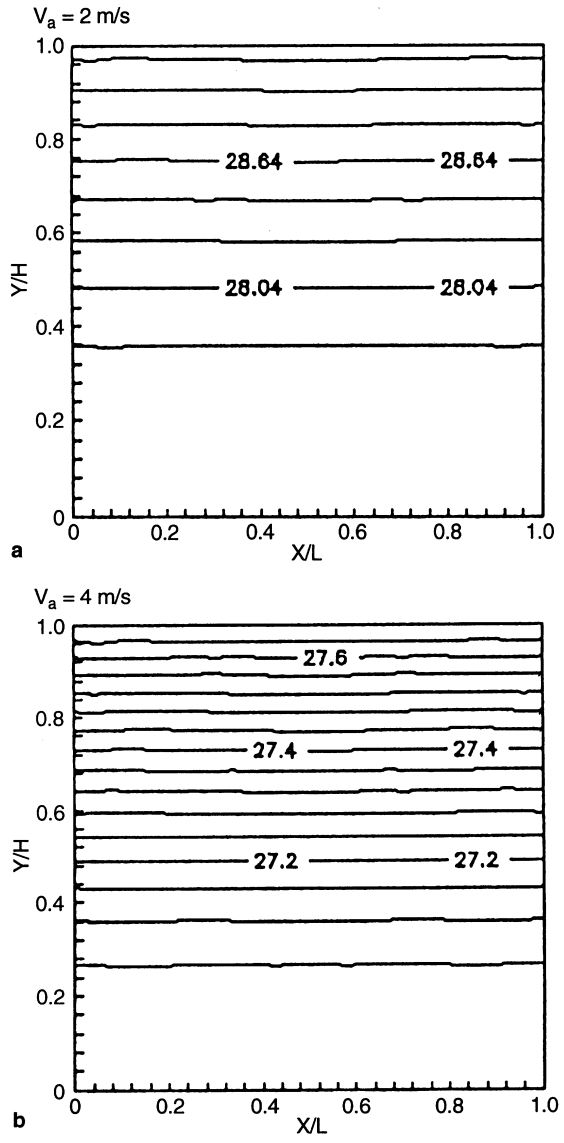

Fig. 5. Temperature contour line (°C) (RH = 60%, Ta = 30 °C, I = 400 W/m^2)

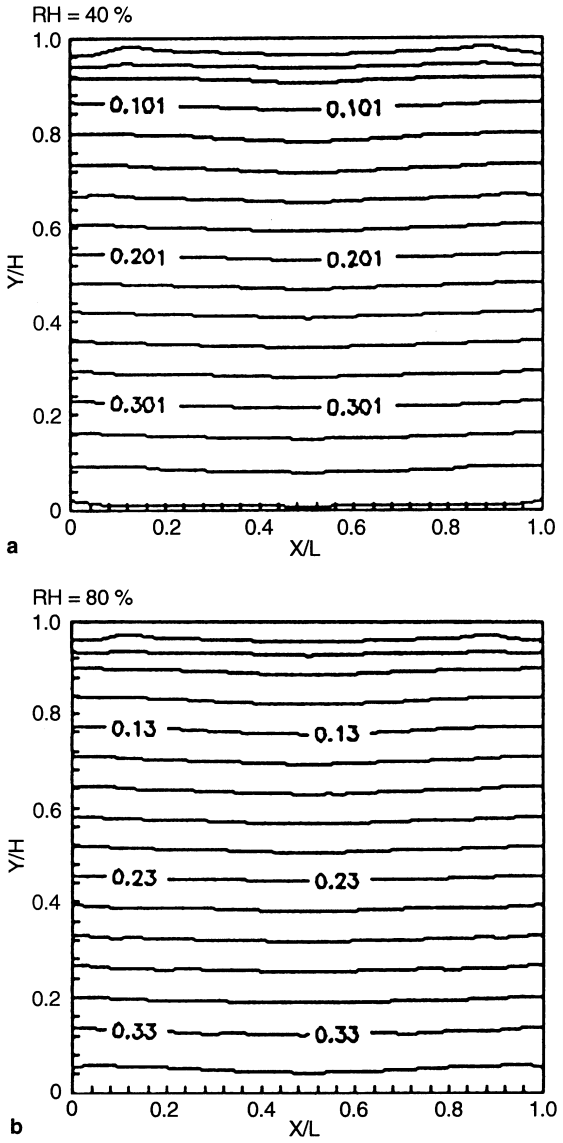

Fig. 6. Water content contour line (%) (Ta = 30 °C, I = 400 W/m^2, Va = 1 m/s)

$$y = H: \quad -k_m \frac{\partial T}{\partial y} = I + h_0(T - T_a) + h_m(\rho_0 - \rho_\infty)\gamma + \varepsilon_s \sigma (T^4 - T_s^4),$$
$$u_l = 0, \quad u_g = v_g = 0. \tag{15}$$

On the bottom boundary of 0.3 meter deep from the upper end, temperature change is quite small, therefore, an adiabatic boundary condition is assumed here. A zero-motion dynamic boundary for gas phase is approximately chosen on the upper surface under atmosphere environment, which be may one of the formative reasons for the natural vortexes of gas mixture in the confined soil bed.

3
Numerical simulations

The governing Eqs. (1–6), together with the boundary conditions (12–15), are solved numerically by finite difference method. The pressure-based algorithm, pioneered by Patankar and Spalding [17, 18], is principally used in our numerical formulations and computations with treating staggered grid in primitive variables and adopting ADI technique for solving the coupled linear equations. There exists no pressure-related term in the liquid-phase momentum equation, only pressure-velocity coupling in gas-phase momentum equation is considered to derive the pressure correction equations through gas-mixture continuity Eq. (2) with a water evaporative term. Water-liquid and water-vapor continuity Eqs. (1, 3) are used for finding water content and water evaporative rate respectively. In order to ensure the convergence of calculation procedure, under-relaxation method is adopted with relaxation factors of 0.1 for water content, 0.5 for velocity, 0.8 for pressure and 0.9 for temperature. As the change rate of water content is not so sensitive to the environment parameters, that a very small relaxation factor is chosen in its iterative calculation for the situation of bottom boundary at a constant water supply.

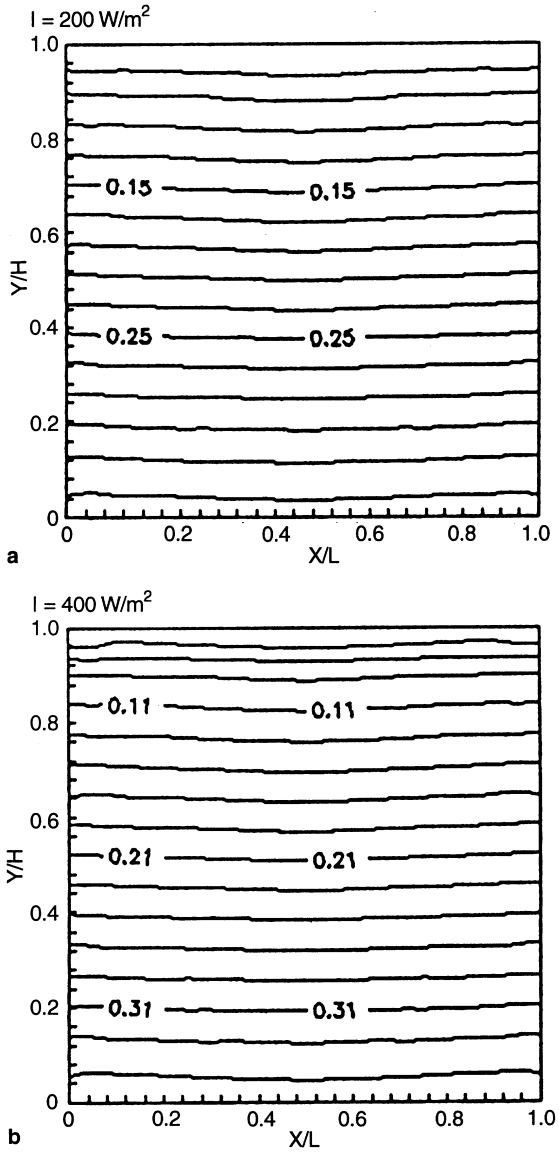

Fig. 7. Water content contour line (%) (RH = 60%, Ta =30 °C, Va = 1 m/s)

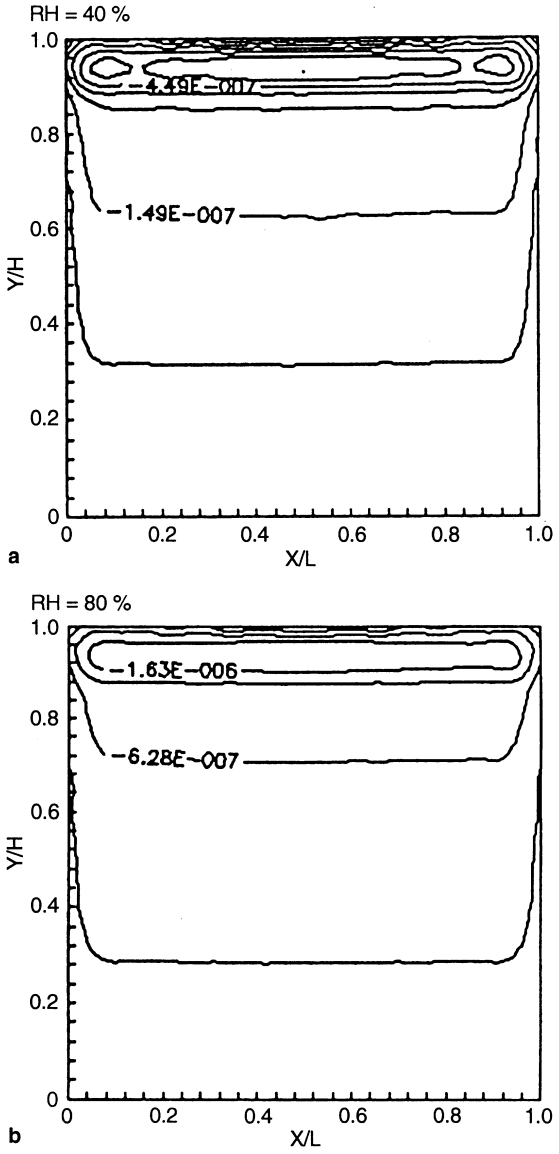

Fig. 8. Water evaporation rate (Kg · m^{-3} · s^{-1}) (Ta = 30 °C, I = 400 W/m^2, Va = 1 m/s)

3.1
Basic parameters

Although the governing equations expressed above is in a general form with vectors, only two-dimensional steady-state simulations are conducted in the present paper. An uniform grid of 25 × 25 is selected in numerical calculation with a cross-section area of 0.3 × 0.3 m^2 for the analysis domain, assuming that one of the horizontal coordinates is infinite. The basic calculating parameters are fixed as: Ambient Temperature Ta = 30 °C; Relative Humidity RH = 60%; Radiative Heat Flux I = 400 W/m^2; Wind Speed Va = 1 m/s.

3.2
Results and discussion

Various influences of the environment parameters on the heat, moisture and gas migrations in the sand-included soil bed with a porosity of $\phi = 38.9\%$ have been studied through the simulating profiles in scalar and vectorial fields which have shown some regularities for understanding the complicated mechanisms in transport phenomena. Appreciable differences in the field distributions changing with environment conditions are discovered through the comparisons in the following figures.

3.2.1
Soil temperature

The temperature of the soil bed is affected by many ambient factors, such as ambient relative humidity RH, ambient temperature Ta, radiative heat flux I, wind speed Va and other climate conditions excluded in this discussion. Off all those atmospheric parameters, the influences of RH, Ta and I are much obvious than others on the field distributions in the soil bed. Figure 2, indicating two-dimensional temperature field, shows the steady-state calculating results in which RH varies from 40 to 80% . Around four degree temperature difference near the upper surface can be told by two contour figures while other ambient conditions keep

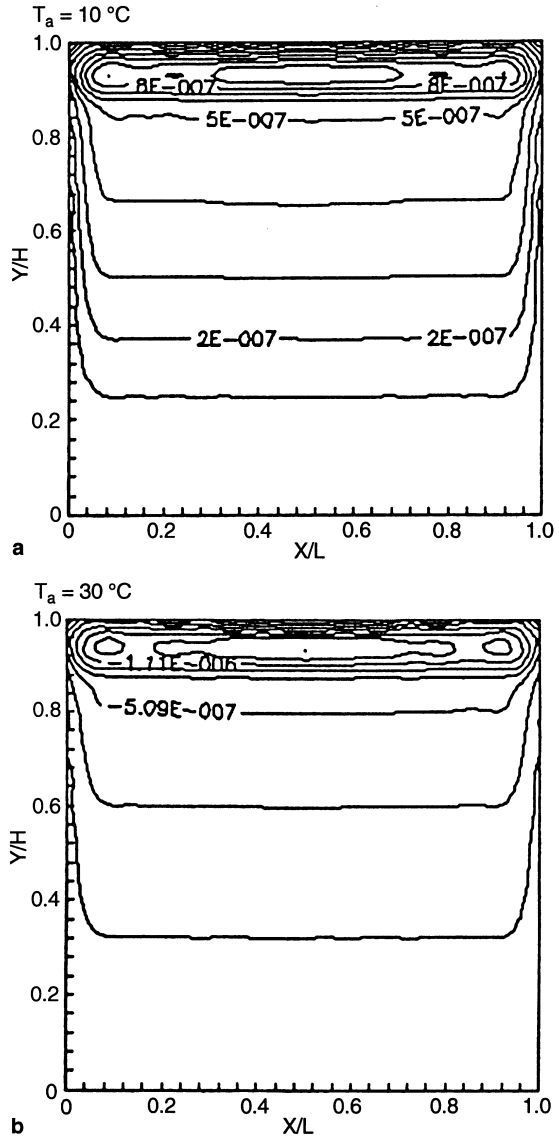

Fig. 9. Water evaporation rate (Kg · m^{-3} · s^{-1}) (RH = 60%, I = 400 W/m^2, Va = 1 m/s)

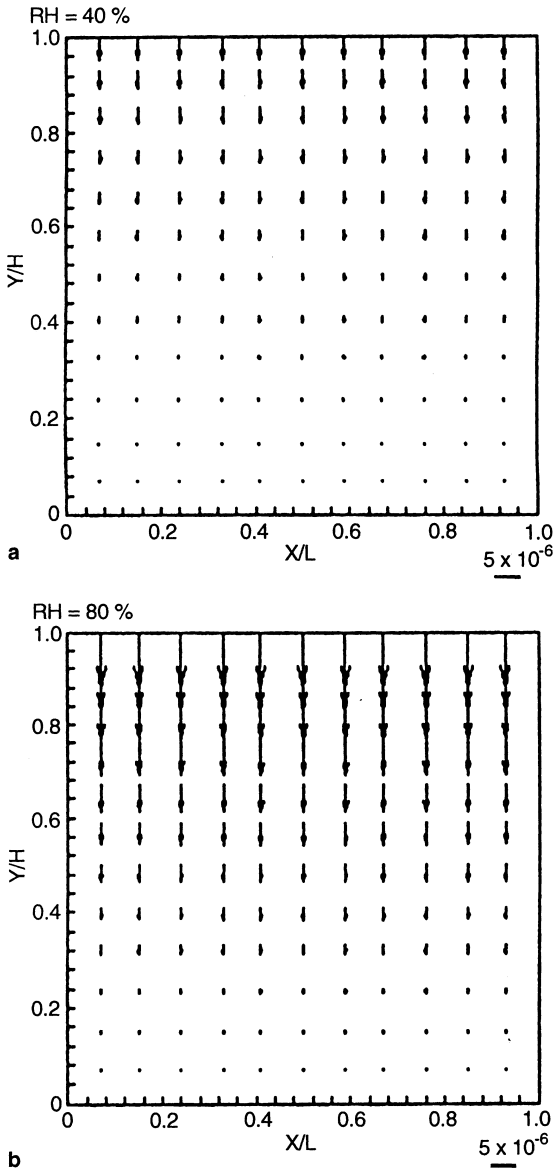

Fig. 10. Vapor velocity vector field (m/s) (Ta = 30 °C, I = 400 W/m^2, Va = 1 m/s)

the same. This may give us some ideas about crop-planting temperature in the dry or the wet climate. When season changes, the soil temperature changes a lot, which can be observed in Fig. 3 with other comparison factors unchanged except the ambient temperature. The amount of incident solar radiation on the earth, depended on a cloudy or clear sky, always changes from time to time, however, a steady radiant flux is assumed in the numerical simulation from 200 to 400 W/m^2, see Fig. 4. The wind speed associated with the heat transfer capacity on the soil surface, as shown in Fig. 5, seems having little action on the temperature propaganda in relatively thicker soil layer for the calculating range of 2–4 m/s.

3.2.2
Soil water content

As mentioned above, we have assumed a constant water supply on the bottom boundary, which might imply that the variation of water content in the soil bed would not be so much as the variation of ambient condition, although it is unusual for a soil deep of 0.3 meter. However, the situation will be totally changed if a kind of irrigation manner could be maintained in this case, and based on the calculating results, the water content difference for RH = 40–80% and I = 200–400 W/m^2 can still be distinguished in Figs. 6 and 7. Our attentions, therefore, are paid to that how ambient relative humidity and solar radiation exert their influences on soil water content, in which we may have some interests for examining the soil moisture in a couple of dry and hot days, while the ambient temperature does not vary a lot. As the driving force for water-liquid migration is mainly the capillary potential, the moisture loss from the evaporation on soil surface can be sufficiently supplemented by a continuous supply from a boundary water source. Consequently, good maintenance for water in soil bed is achieved.

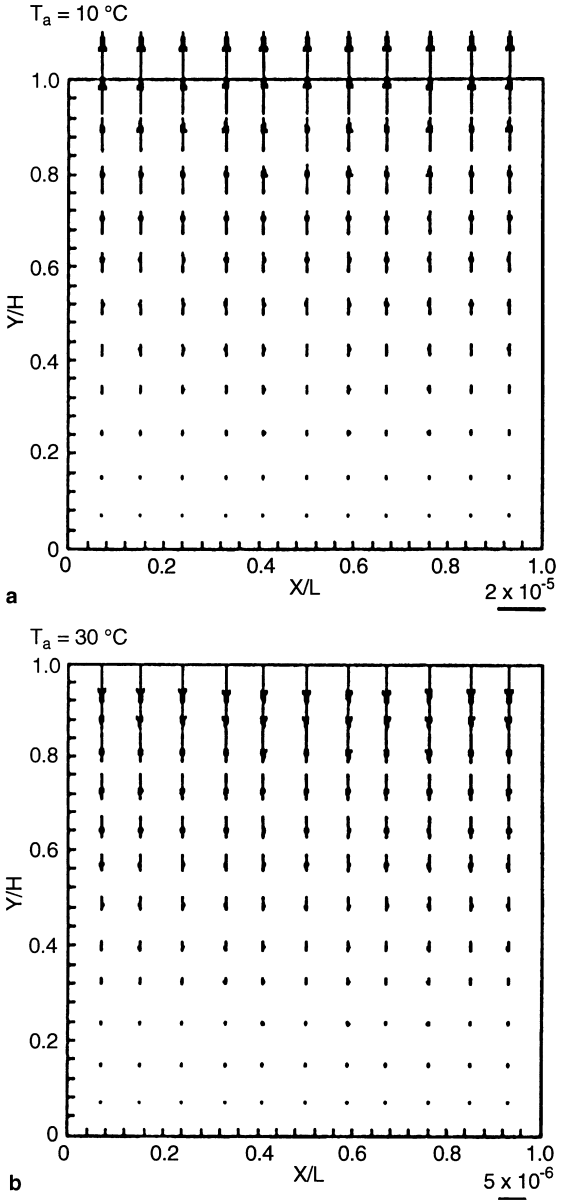

Fig. 11. Vapor velocity vector field (m/s) (RH = 60%, I = 400 W/m^2, Va = 1 m/s)

3.2.3
Soil water evaporation

The phase changes of water inside soil bed, which could be either evaporation or condensation, differ from various situations. At the ambient temperature of 30 °C, a condensation-dominated phase-change process, with a negative evaporation rate, has been observed in Fig. 8 when RH = 40–80%. Nevertheless, at a relatively lower ambient temperature, say 10 °C, an evaporation-controlled phase-change process can be found from Fig. 9 with a positive evaporation rate, when RH = 60%. What a phase-change process is, in general, depended on the direction of heat flux in the wet soil, not on the temperature level which, however, is related to the phase-change rate. According to the figures we could see that: (1) the lower the relative humidity, the stronger the water evaporation is, and (2) the higher the relative humidity, the stronger the water condensation is in the confined soil bed.

3.2.4
Vapor velocity

We have to evaluate the diffusivity motion of water vapor by Eq. (11), because its order of magnitude is not smaller than that of the bulk motion of gaseous mixture. Besides, the motive direction of water vapor can determine whether a evaporation or a condensation process in the soil bed. The comparison is made in Fig. 10, with the same calculating parameters as they have in Figs. 2 and 8, when RH varies from 40 to 80%, between which the condensation rates are quite different. In order to meet the mass balance, in this case, there must be a condensation process, due to a downward vapor motion. But when happens a upward vapor motion, in another case displayed in Fig. 11, then appears an evaporation process at Ta = 10 °C. This phe-

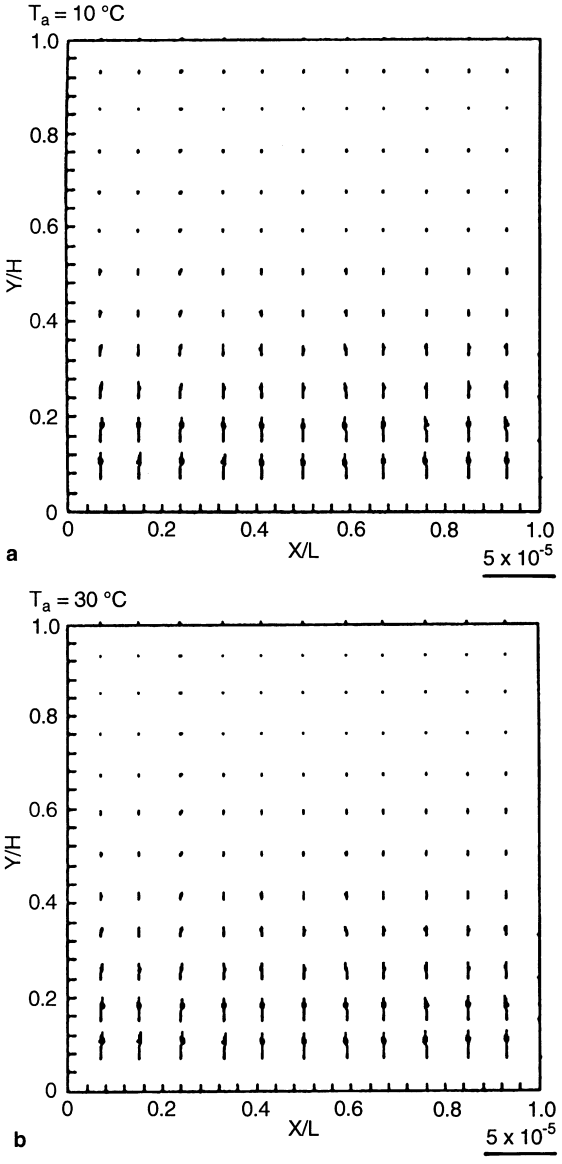

Fig. 12. Liquid velocity vector field (m/s) (RH = 60%, I = 400 W/m^2, Va = 1 m/s)

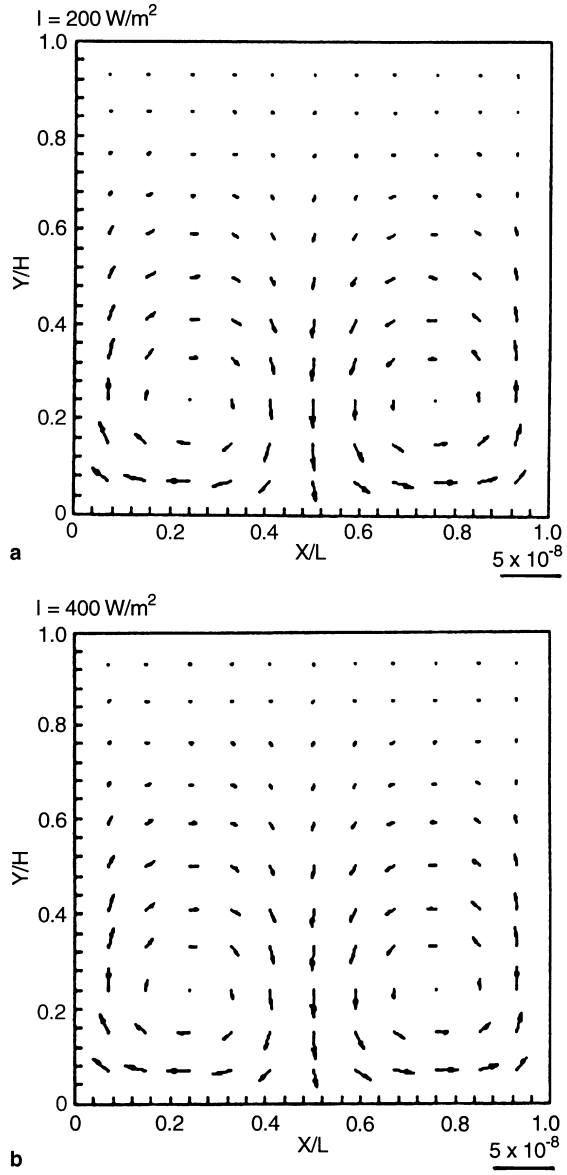

Fig. 13. Gas velocity vector field (m/s) (RH = 60% , Ta = 30 °C, Va = 1 m/s)

nomena can be explained by Eq. (11), as the temperature gradient in the first term of right-hand side, being positive or negative, is a dominated factor. The water content gradient is always negative, and not sensitive to the motive direction of water vapor in the situation we have considered.

3.2.5
Liquid and gas velocities

Both velocities of liquid- and gas-phase are not getting big changes under the investigated ambient conditions. One may see, in Fig. 12 with Ta = 10–30 °C, that the water liquid keeps its motive direction upward in whatever calculating conditions, as long as the evaporation maintains on the earth surface. Just little change in velocity of water liquid is found, as the surface evaporation is not so strong for current calculating conditions. The gaseous velocity also shows a little change for the range of I = 200–400 W/m^2 in Fig. 13. Two symmetric vortexes are formed in each of cases, although they are relatively weak, due to the natural convection of gaseous mixture in the confined porespace, as the consequence of momentum movement balanced by various force terms in Eq. (5).

To sum up, we have seen connections among the soil temperature, the heat flux and the moisture transfer from above simulations rather numerically-oriented. As the actions of high ambient temperature and solar radiation, the soil obtains heat, and the surface temperature of the soil bed rises, while the water evaporation on the soil surface can decreases this temperature level for high soil water content. Inside soil bed, the temperature gradient influences the moisture transfer that also affects the heat flux through evaporation in return, however, the moisture migration is dominated by water evaporation on soil surface in its liquid state, and by temperature gradient in its vapor state.

4
Conclusions

The governing equations presented in this paper is suitable for describing simultaneous heat, moisture and gas migrations in soil with or without the presence of plant roots due to its theoretical completeness and numerical solubility. A satisfied image on transport phenomena in a confined soil bed is provided with the field distributions of various variables which will represent multiphase flow and heat transfer characteristics. The atmospheric environment exerts significant effects on transport processes in soil, but ambient temperature, relative humidity and solar radiation play more important roles than others based on the steady numerical simulations in two-dimension.

References

1. **Philip JR; DeVries DA** (1957) Moisture movement in porous materials under temperature gradients. Trans Am Geophys Union 38: 222–232
2. **Luikov AV** (1966) Heat and Mass Transfer in Capillary Porous-Bodies. Oxford: Pergamon Press
3. **Slattery JC** (1970) Two-phase flow through porous media. AIChE J 16: 345–354
4. **Whitaker S** (1977) Simultaneous heat, mass and momentum transfer in porous media: a theory of drying. Advances in Heat Transfer. New York: Academic Press
5. **Eckert ERG; Faghri M** (1980) A general analysis of moisture migration caused by the temperature differences in an unsaturated porous medium. Int J Heat Mass Transfer 23: 1613–1623
6. **Udell KS** (1983) Heat transfer in porous media heated from above with evaporation, condensation and capillary effects. ASME J Heat Transfer 105: 485–492
7. **Vafai K; Tien HC** (1989) A numerical investigation of phase change effects in porous materials. Int J Heat Mass Transfer 32: 1261–1277
8. **Cheng P; Pei DCT** (1989) A mathematical model of drying process. Int J Heat Mass Transfer 32: 297–310
9. **Camillo PJ; Curney RJ; Schmugge TJ** (1983) A soil and atmospheric boundary layer model for evapotranspiration and soil moisture studies. Water Resour Res 19: 371–378
10. **Milly PCD** (1984) A simulation analysis of thermal on evaporation from soil. Water Resour Res 20: 1087–1098
11. **Gray WG; Hassanizadeh SM** (1991) Unsaturated flow theory including interfacial phenomena. Water Resour Res 27: 1855–1863

12. **Sarkar S; Kar S** (1995) Comparison between simulated and measured profile water distribution. Agric Water Manage 27: 341–350
13. **Liu W; Zhao XX; Luo XB; Huang SY; Mizukami K** (1997) Numerical Simulation of Heat and Mass Transfer in Soil. Proc. 10th Int. Symp. on Transport Phenomena 3: 919–923
14. **Liu W; Peng SW; Mizukami K** (1995) A general mathematical modeling for heat and mass transfer in unsaturated porous media: an application to free evaporative cooling. Heat and Mass Transfer 31: 49–55
15. **Liu W; Peng SW; Mizukami K** (1997) Moisture Evaporation and Migration in Thin Porous Packed Bed Influenced by Ambient and Operating Conditions. Int J Energy Research 21: 41–53
16. **Liu W; Zhao XX; Huang SY; Zhang Z** (1997) The model of heat and moisture transport in HIPAS system. (in Chinese) J Huazhong Univ Sci Technol 25: 1–7
17. **Patankar SV** Numerical Heat Transfer and Fluid Flow. Washington DC: Hemisphere 1980
18. **Patankar SV; Spalding DB** (1972) A calculation procedure for heat, mass and momentum transfer in three-dimensional parabolic flows. Int J Heat Mass Transfer 15: 1787–1806